JOURNAL OF GEOPHYSICAL RESEARCH, VOL. 86, NO. C9, PAGES 8075–8084, SEPTEMBER 20, 1981

Measurements of a Saturated Range in Ocean Wave Spectra

GEORGE Z. FORRISTALL

Shell Development Company, Houston, Texas 77001

Wavestaff measurements made in the Gulf of Mexico and Waverider measurements from the Baltimore Canyon area have been used to study the form of ocean wave spectra at high frequencies. The observations are statistically consistent with the idea that the tail of the spectrum is in equilibrium with the local wind. Analysis showed that the spectral range between the mean wave frequency and about two and one half times that frequency is consistently proportional to the inverse of the fourth power of the frequency. At higher frequencies, the classical inverse fifth power law seems to hold. In the inverse fourth power range, the amplitude of the spectrum is also proportional to the wind friction velocity. These relationships should permit a reliable specification of this saturated range when only local wind observations are available. If the significant wave height and mean period are known, the amplitude of the tail of the spectrum can be predicted with somewhat greater accuracy. However, this relationship should be used with caution when the height and period statistics are influenced by swell.

INTRODUCTION

To a good degree of approximation, a record of wind-generated waves can be described as filtered white noise. Thus, the essential product of wave prediction schemes is the wave power spectrum. These prediction models are generally quite complicated since they must account for the propagation of the waves through wind fields that vary in space and time. However, it has often been observed that a substantial portion of the spectrum above the frequency of the spectral peak is saturated and in equilibrium with the local wind.

The specification of the saturated range of the spectrum is an important part of any wave prediction scheme. In recent years, the construction of fixed structures in deep water has increased the practical need for knowledge of this range. If the natural periods of the structure are long enough, substantial fatigue damage may be caused by many repetitions of relatively small waves. The fatigue analysis of the Cognac platform by *Kinra and Marshall* [1979] showed that high cycle fatigue could be significant even in the mild Gulf of Mexico climate.

The wave frequencies of most importance in fatigue problems generally lie in the saturated range. Thus, it should be possible to hindcast the necessary portion of the wave spectral climate, using relatively simple formulas. In most cases, the starting point for the hindcasts will be wind statistics, but in some areas, the average wave height and period climate may be known. If these statistics are not too much influenced by the presence of swell from distant storms, they may permit a specification of the saturated range that is more accurate than that based on only wind data.

The purpose of this paper is to examine a large body of wind and wave measurements and develop functional forms for the portion of the wave spectra observed to fall in the saturated range. We begin by describing the sources of wind and wave data that include measurements in the Gulf of Mexico and the Atlantic Ocean made by wavestaffs and a Waverider buoy. Wave spectra calculated from these measurements are put into nondimensional forms and compared with the available theory and with previously reported measurements. A substantial portion of the saturated range is found to depend on the wind friction velocity. The saturated range was also determined as a function of significant wave height and period for a portion of the data in which the contribution of swell was small.

DATA SOURCES

The wind and wave measurements were made over a number of years in conjunction with oil exploration and production activities on the continental shelves of the United States. In all of the measurement projects involved, repeated calibrations were performed to maintain good data quality under difficult field conditions. From these data sets, we selected segments that covered a wide range of conditions. The most pertinent details of the measurement site locations and instrumentation are listed in Table 1.

The Ocean Data Gathering Program (ODGP) collected wind and wave data at six sites in the northern Gulf of Mexico from 1968 through 1971. The instrumentation, which basically consisted of Bendix aerovanes and Baylor wavestaffs recorded on Geotech tape recorders, was described by *Patterson* [1974]. *Ward* [1974] and *Hamilton and Ward* [1974] give an overview of the results of the program.

The measurements used in this study were made at ODGP station 1, located in South Pass block 62, from August to November 1970 and June and July 1971. Before August 1970, the anemometer at the site was rather badly shielded, and many data segments from the times listed above were removed through various quality checks. However, since one spectrum based on 20 min of data was available for each hour of good data, there were still 1270 spectra available for analysis.

Drawing on experience gained in the ODGP, the Ocean Current Measuring Program (OCMP) used the same basic instrumentation system with the addition of a string of electromagnetic current meters [*Forristall and Hamilton,* 1978]. Measurements were made at three stations in the northern Gulf of Mexico from 1972 through 1977. Data from hurricanes Eloise and Anita was of high quality, included a wide variety of wind speeds, had already been converted to digital format, and was therefore used in this study. Some aspects of the directional wave spectra in hurricane Eloise have already been discussed by *Forristall et al.* [1980]. Measurements at station 2 (EI331) were made with a Baylor wavestaff and J-TEC vortex shedding anemometer, and measurements at station 3 were made with another Baylor wavestaff and a Bendix aerovane. Each hurricane data set included 300–600 spectra.

From April 1978 through February 1979, the Western Pace-

Paper number 1C0848.
0148-0227/81/001C-0848$01.00

TABLE 1. Measurement Station Locations and Instrumentation

	South Pass 62	Eugene Island 331	Pacesetter
Latitude	29°15′N	28°14′N	39°20′N 38°42′N*
Longitude	88°44′W	91°42′W	73°06′W 73°32′W*
Water depth (m)	99	75	63
Wave	wavestaff	wavestaff	Waverider
Wind	aerovane	J-TEC	aerovane
Anemometer height (m)	50 (ODGP) 40 (OCMP)	44	61

* After July 10, 1978.

setter II drilled three exploratory wells in the Baltimore Canyon area approximately 100 miles off the coast of New Jersey. An aerovane, Waverider buoy, and an automatic digital recording system were used to obtain wind and wave data during most of the drilling program [*Forristall*, 1980]. One 20-min data segment was recorded every 3 hours on a digital cassette tape. After bad data segments were eliminated, 1027 data segments obtained in a wide variety of meteorological conditions remained.

The data set thus includes measurements from wavestaffs and buoys in a wide variety of meteorological conditions including hurricanes, East Coast winter storms, and relatively mild Gulf Coast conditions. Conclusions that are common to all the data sources should be quite convincing.

Any study of the behavior of the wave spectrum over a reasonably wide frequency range depends heavily on the linearity of the wave sensor and recording system. Our static calibrations of the staffs used have typically shown linearity to within 1–2%. The staff will follow level changes at rates on the order of 300 m/s, so there should be no electronic limitation to its frequency response for the wave periods of interest. The main limitation of the staff itself in the study of high frequency waves seems to be the 25 cm spacing between its two cables. A 1.5 m long sinusoidal wave propagating parallel to the plane of the cables would have its measured amplitude lowered by 10% due to the spacing of the cables; the error for a 3m long wave would be only 3%.

The wavestaffs were mounted on oil production platforms whose members might cause some interference with the incident wave field. A platform leg in a long wave causes a disturbance of the surface with dimensions comparable to the diameter of the leg. When the wave passes, this disturbance will radiate away as free waves of relatively high frequency. *Forristall et al.* [1979] ascribed differences between measurements made by a Waverider and a wavestaff mounted on a semisubmersible drilling rig to this type of effect and found that the discrepancy became noticeable for frequencies higher than those corresponding to waves twice as long as the 10-m diameter of that rig's columns. The platforms used in this study have typical leg sizes of about 1.5 m, so if the size of the radiated waves scales as the diameter of the member, there should be no errors for wave frequencies less than about 0.7 Hz.

The recorders used with the wavestaffs were tested and found to have a flat frequency response to 3 Hz and down 1 dB at 4 Hz. In summary, there seems to be no systematic source of errors in the wavestaff-recorder system for waves with frequencies less than about 0.7 Hz.

The limiting factor in the high frequency response of the Waverider system is the hydrodynamic response of the 0.7-m diameter buoy to short waves. This response depends somewhat on the details of the mooring, but it is substantially flat to 0.5 Hz, after which it rises to a peak at 0.8 Hz and then rapidly declines. Since the recording system for the buoy was digital, it is more naturally discussed in the next section.

DATA PROCESSING

All the measurements discussed in the previous section were converted to digital form for processing. Spectral estimates were then made by applying a Fast Fourier Transform (FFT) and averaging over bands in the frequency domain.

The digitization rate for the ODGP data was 3.44 Hz, and an eighth-order anti-aliasing filter with a 4 dB point at approximately 0.8 Hz was used. The spectra were calculated by taking an FFT over 4096 points that corresponds to about 20 min of data. The raw spectra were then averaged over the frequency bands listed in Table 2. Note that the width of the bands and thus the stability of the estimates varies with frequency. The highest two bands were not used in this study because of possible problems with the response of the system at those high frequencies.

The digitization rate for all the OCMP data sets was 2.0 Hz and a four-pole anti-aliasing filter with a 3 dB point at 0.8 Hz was used. Spectra were calculated by taking an FFT over 2048 samples, and the raw spectra were averaged over 10 adjacent frequency bands, giving a width of 0.0098 Hz for each averaged band.

The Waverider data from the Baltimore Canyon were recorded on a digital cassette system similar to that described by *Alexander and Hamilton* [1978]. The digitizing rate for the wave data was 2.0 Hz, and a four-pole anti-aliasing filter with a 3 dB point at 0.66 Hz was used. The spectra were calculated with the method used for the OCMP data.

The wind data were also digitized prior to analysis, but the details are not important since the data were used only to form 20-min vector averages of speed and direction. Since wind speed varies with height, the anemometer height must be taken into account when comparing data from various sources. The variation of wind speed can be described by a logarithmic law of the form

$$u = (u_*/\kappa) \ln (z/z_o) \quad (1)$$

where u is the wind speed at height z, $\kappa = 0.41$ is von Karman's constant, u_* is the friction velocity, and z_o is the roughness length. The friction velocity and roughness length are scaling parameters for the logarithmic profile that give characteristic velocity and length scales in the boundary layer. *Garratt* [1977] reviewed the available observations and concluded that for a neutrally stable atmosphere over the ocean, the friction velocity and roughness length could be related by

$$z_o = 0.0144\, u_*^2/g \quad (2)$$

where g is the acceleration of gravity. If the wind speed at some elevation z has been measured, equations (1) and (2) may be solved by iteration to give u_* and z_o and the wind speed at any other elevation found from (1).

All our wind measurements were reduced to the rather peculiar height of 19.5 m for the historical reason that the anemometers on the *Weather Explorer* and *Weather Reporter* were at this height, and the Pierson-Moskowitz spectrum was developed by using data from those ships. However, it turned out in the analysis that the friction velocity itself was more

TABLE 2. ODGP Spectral Analysis Bands

Band	Upper Frequency	Period of Upper Frequency	Center Frequency	Period of Center Frequency	Number of Estimates in the Band
1	0.0403	24.82	0.0201	49.64	48
2	0.0504	19.86	0.0453	22.06	12
3	0.0554	18.05	0.0529	18.91	6
4	0.0621	16.10	0.0588	17.02	8
5	0.0713	14.02	0.0667	14.99	11
6	0.0772	12.95	0.0743	13.46	7
7	0.0831	12.03	0.0802	12.47	7
8	0.0873	11.46	0.0852	11.74	5
9	0.0907	11.03	0.0890	11.24	4
10	0.0948	10.54	0.0928	10.78	5
11	0.0999	10.01	0.0974	10.27	6
12	0.1049	9.53	0.1024	9.77	6
13	0.1108	9.03	0.1079	9.27	7
14	0.1175	8.51	0.1142	8.76	8
15	0.1251	8.00	0.1213	8.24	9
16	0.1335	7.49	0.1293	7.74	10
17	0.1427	7.01	0.1381	7.24	11
18	0.1536	6.51	0.1482	6.75	13
19	0.1670	5.99	0.1603	6.24	16
20	0.1821	5.49	0.1746	5.73	18
21	0.1998	5.01	0.1910	5.24	21
22	0.2224	4.50	0.2111	4.74	27
23	0.2501	4.00	0.2363	4.23	33
24	0.2854	3.50	0.2678	3.73	42
25	0.3332	3.00	0.3093	3.23	57
26	0.4004	2.50	0.3668	2.73	80
27	0.5003	2.00	0.4503	2.22	119
28	0.9997	1.00	0.7500	1.33	595
29	1.7182	0.58	1.3590	0.74	856

useful as a parameter than the speed at any particular reference level.

The relationship between roughness length and friction velocity is known to be dependent on atmospheric stability, which in turn depends on the air-sea temperature difference. Thus, there is some question whether it is appropriate to apply (2) to all our data. However, the hurricane measurements were made under conditions of near-neutral stability, and the importance of the stability parameter decreases with increasing wind speed. Since the air-sea temperature difference would in general not be known in the application of our results to a fatigue study, it is in any case useful to know how well the spectrum may be specified when this information is not used.

NONDIMENSIONAL SPECTRA AND THE EQUILIBRIUM RANGE

Dimensional analysis has proved to be a valuable tool in the study of wave spectra. The spectral density $S(f)$ has dimensions L^2T. If, following *Kitaigorodskii* [1973], we assume that the only variables influencing the form of the spectrum are gravity, the wind velocity, and the fetch of the wind x, then on dimensional grounds the spectrum must have the form

$$S(f) = g^2 f^{-5} F(\bar{f}, \bar{x}) \qquad (3)$$

where the dimensionless frequency and fetch groups are given by

$$\bar{f} = fu/g \qquad (4)$$

and

$$\bar{x} = xg/u^2 \qquad (5)$$

The JONSWAP spectrum devised by *Hasselman et al.* [1973] has proven useful for describing a wide variety of wave spectra. It is given by

$$F(\bar{f}, \bar{x}) = \alpha(2\pi)^{-4} \exp\{-1.25(\bar{f}/\nu)^{-4} + \ln\gamma \exp[-(\bar{f}/\nu - 1)^2/2\sigma^2]\} \qquad (6)$$

where the parameters α, ν, γ, and σ are all functions of the nondimensional fetch $\bar{x}$. In this equation

$$\bar{f}/\nu = f/f_m \qquad (7)$$

where f_m is the frequency of the spectral peak, α is the Phillipps constant, γ is the peak enhancement factor, and σ describes with width of the spectral peak.

The functional dependence on fetch describes the growth of the spectrum under the continued action of the wind. This growth cannot continue indefinitely. For long fetches and durations, the energy input is balanced by dissipation and transfer processes so that the spectrum reaches a limiting form. The *Pierson and Moskowitz* [1964] spectrum for fully developed seas is given by (6) with $\gamma = 1$ and α and ν constant.

Even if the entire spectrum is not fully developed, some range of its high frequency tail may become saturated relatively quickly, so that it is essentially in balance with the local wind. Knowledge of the extent and form of such an equilibrium range is of practical importance, since it could be predicted without extensive knowledge of the windfield.

Hasselman et al. [1973] gave persuasive arguments for the use of the wind speed at 10-m height in (4) and (5). However, it is also possible to form the nondimensional groups by using the wind friction velocity, and one could argue that this choice is more appropriate for the study of the local energy balance. In

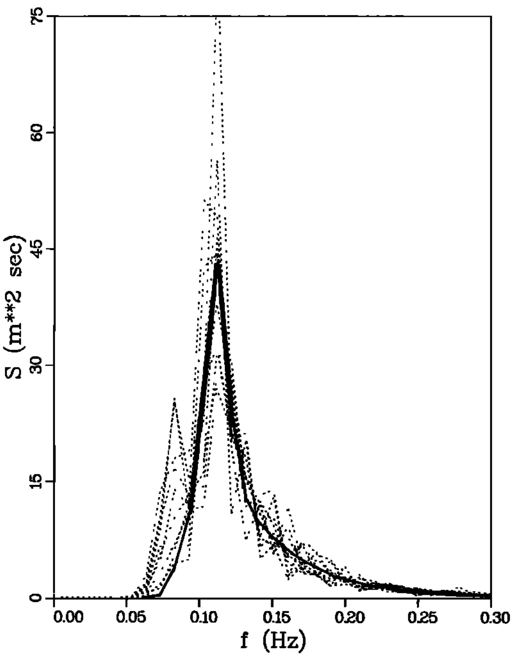

Fig. 1. Individual spectra from SP62 during hurricane Eloise for 19.5 m winds between 22.4 and 24.6 m/s are shown by dotted lines. The solid line is the JONSWAP parameterization discussed in the text.

practice, our data in the equilibrium range was described much more consistently when the friction velocity was used. The nondimensional frequency is then

$$\tilde{f} = fu_*/g \tag{8}$$

and if a nondimensional spectrum is defined by

$$\tilde{S}(\tilde{f}) = S(f)g^3/u_*^5 \tag{9}$$

then

$$\tilde{S}(\tilde{f}) = \tilde{f}^{-5}F(\tilde{f}) \tag{10}$$

Phillips [1977, p. 144] simplified the equation further by postulating a range for which the friction velocity is unimportant and the spectrum is limited only by breaking under the influence of gravity. The function $F(\tilde{f})$ then must be a constant, and

$$S(f) = \alpha(2\pi)^{-4}g^2f^{-5} \tag{11}$$

The dimensional analysis shows that the shape of the nondimensional spectrum is related to its functional dependence. As noted above, if the saturated range is independent of friction velocity, the spectrum will be proportional to f^{-5}. Inversely, if the saturated range is found to have some other power law relationship, it must also depend on the wind friction velocity.

MEASURED SPECTRA

Over 4000 spectra were computed in this study, so only a small sample of the individual spectra can be presented. Figure 1 shows one of the more interesting subsets: the spectra from SP62 during Eloise for the times when the 19.5m wind was beween 22.4 and 24.6 m/s. The peaks near 0.08 Hz are clearly swell, but the rest of each spectrum can be described rather well by the JONSWAP parameterization. The solid line in Figure 1 was calculated from (6) with f_m = 0.112, α = 0.0144, γ = 3.0, and σ = 0.08. These parameters were obtained by fitting the ensemble average of the individual spectra in the range between 0.09 and 0.20 Hz. Any single spectrum could be better fit by changing the shape parameters γ and σ. The frequency of maximum energy could be obtained from the formulas of *Hasselman et al.* [1973] by choosing a fetch equal to 135 km. Although it is difficult to determine objectively the fetch in the decidedly nonhomogeneous windfield of a hurricane, this value is certainly reasonable.

The individual spectra in Figure 1 are rather widely scattered, but as statistics of a random process, they are expected to display some variation. If the wave elevation were normally distributed and the population were homogeneous, the spectral densities should have a chi-squared distribution with 20 degrees of freedom. The scatter due to this natural variability is substantial: For 20 degrees of freedom, the expected ratio of the standard deviation to the mean spectrum is 32%.

A Kolmogorov-Smirnov (KS) test was performed to determine the probability that the spectra were drawn from a chi-squared distribution with the proper number of degrees of freedom and thus by inference came from a homogeneous population. To perform the test, the maximum absolute difference between the sample distribution and the chi-square distribution was found and compared to the critical values for the KS test given, for example, by *Hoel* [1962].

The spectra shown in Figure 1 passed the KS test for all frequencies greater than 0.09 Hz. An ensemble average of the spectra in this frequency range is thus representative of the data set even though the windfield in the hurricane was complex and rapidly changing. The dashed line in Figure 2 shows the ensemble average of the data from Figure 1, multiplied by f^5/g^2 to emphasize the details of the high frequency tail. The solid line in Figure 2 is the same JONSWAP spectrum as given in Figure 1. It fits the average data well up to about 0.23 Hz, but lies below the data at higher frequencies. The shape of a Pierson-Moskowitz spectrum is the same as the JONSWAP except that it lacks the enhanced peak at 0.122 Hz. However, the usual Pierson-Moskowitz α-0.081 would underestimate the high frequency data badly, and since the measured spectrum

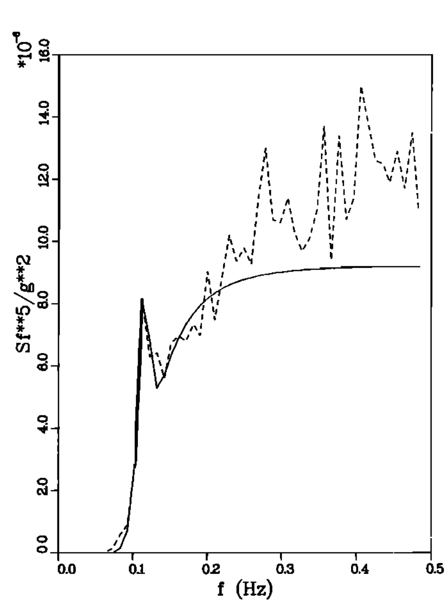

Fig. 2. The dashed line is the ensemble average of the measured spectra in Figure 1. The solid line is the JONSWAP spectrum.

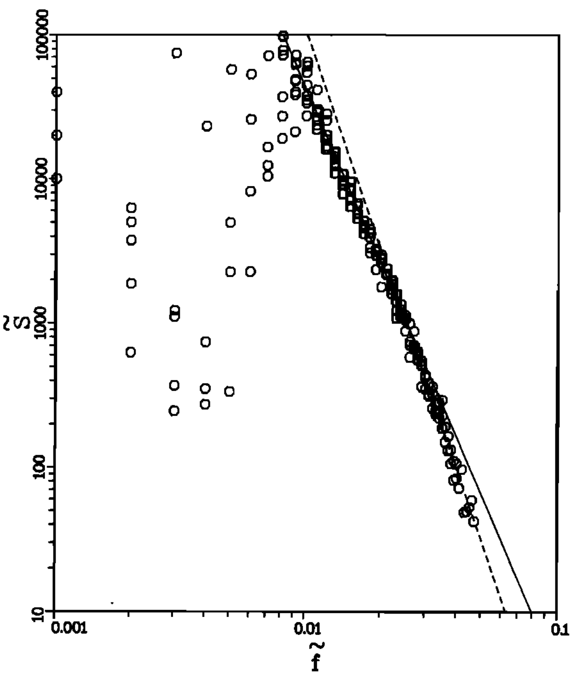

Fig. 3. Nondimensional spectra from the Pacesetter data. The solid line has a slope of −4 and the dashed line has a slope of −5 with the scale factor given in Table 3.

is not fully developed, the Pierson-Moskowitz peak frequency of 0.058 Hz is much too low.

The spectra from different wind speed ranges can best be compared in their nondimensional form. The spectra from each station were first collected in 2.24 m/s wide wind speed ranges. The friction velocity for the 20-min average wind was found by using (1) and (2) and the nondimensional frequencies and spectral densities were found by using (8) and (9). Then the ensemble average of the spectra in each wind speed category was calculated.

At the 90% confidence level, almost all the OCMP hurricane spectra passed the KS test for nondimensional frequencies greater than 0.01, and the spectra generally passed the test for $\tilde{f} > 0.008$. The Pacesetter data passed the test only for wind speeds greater than 8.9 m/s and $\tilde{f} > 0.01$ and the ODGP data never passed the test. The particularly good behavior of the hurricane data may reflect the fact that each data set comes from a single storm. On the other hand, the poor behavior of the ODGP data may be due to some of the spectra being fetch limited. It is interesting to note that the requirement that the wind speed be constant for 3 hours did not substantially improve the homogeneity of the data.

Since the spectra cover a wide range and a power law relationship is indicated by (10), it is convenient to first display the data on log-log plots. Figures 3 and 4 show the nondimensional spectra in this form from the data sets for the Pacesetter and Eloise at South Pass 62. The average spectrum for each wind speed category was plotted separately to determine whether the nondimensionalization properly accounted for different wind speeds. Note that the range of nondimensional frequencies covered by the data increases with friction velocity.

Several features are immediately evident. For nondimensional frequencies above about $\tilde{f} = 0.01$, the spectra for various wind speeds have little scatter, showing that the nondimensionalization is effective and suggesting that there does exist an equilibrium range, which may be effectively described by equation (10). The similarity between the data sets and the homogeneity of the individual spectra discussed above support the same conclusion.

A nondimensionalization based on the wind speed at the 19.5 m reference level instead of on the friction velocity resulted in noticeable separation between wind speed categories. The better fit by using the friction velocity is particularly notable since it was calculated by using the questionable assumption of neutral stability. The friction velocity thus seems to be fundamentally related to the processes that establish the saturated range.

At frequencies lower than $\tilde{f} = 0.01$, the scatter increases greatly, indicating that this portion of the spectrum is no longer in equilibrium with the local wind. In particular, the scatter could be caused by fetch or duration limitation of the spectrum or swell propagating from distant wind systems. The two straight lines shown on the figures have slopes of −4 and −5, corresponding to $\tilde{f}^{-4}$ and $\tilde{f}^{-5}$ power laws. The data for $0.01 < \tilde{f} < 0.025$ seem to be much better described by an $\tilde{f}^{-4}$ law. An $\tilde{f}^{-5}$ dependence only becomes apparent for $\tilde{f} > 0.03$.

The portions of the spectra that follow a power law dependence can be effectively studied on another type of graph where the spectra are multiplied by a power of the frequency. Figures 5–7 show three of the data sets multiplied by $\tilde{f}^4$ and Figures 8 and 9 show two other data sets multiplied by $\tilde{f}^5$. Linear scales are used in all these figures. The $\tilde{f}^5$ graphs show the behavior of the function $F(\tilde{f})$ defined in (10), with a horizontal trend indicating that the simplification of (11) is appropriate, while the horizontal trends on the $\tilde{f}^4$ plots indicate that the spectrum is proportional to $\tilde{f}^{-4}$. The wind speed categories are denoted by the various symbols, and it is again obvious that the nondimensionalization used effectively accounts for the influence of wind speed variations.

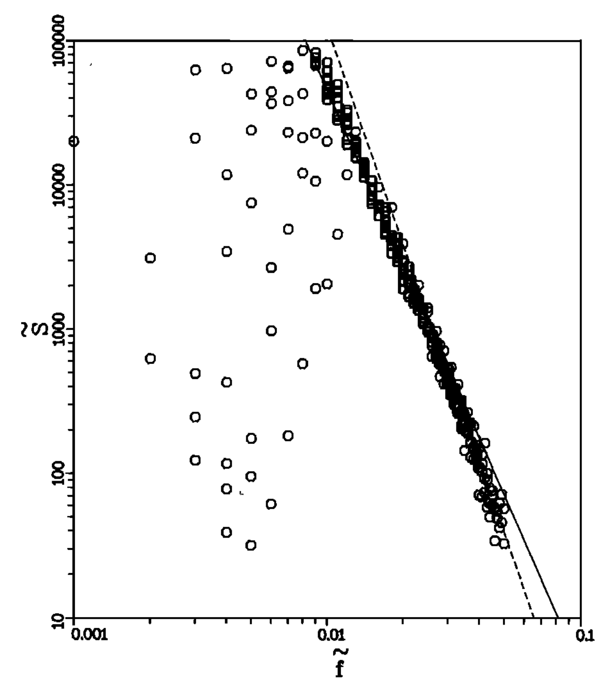

Fig. 4. Nondimensional spectra from Eloise at South Pass 62. Legend as in Figure 3.

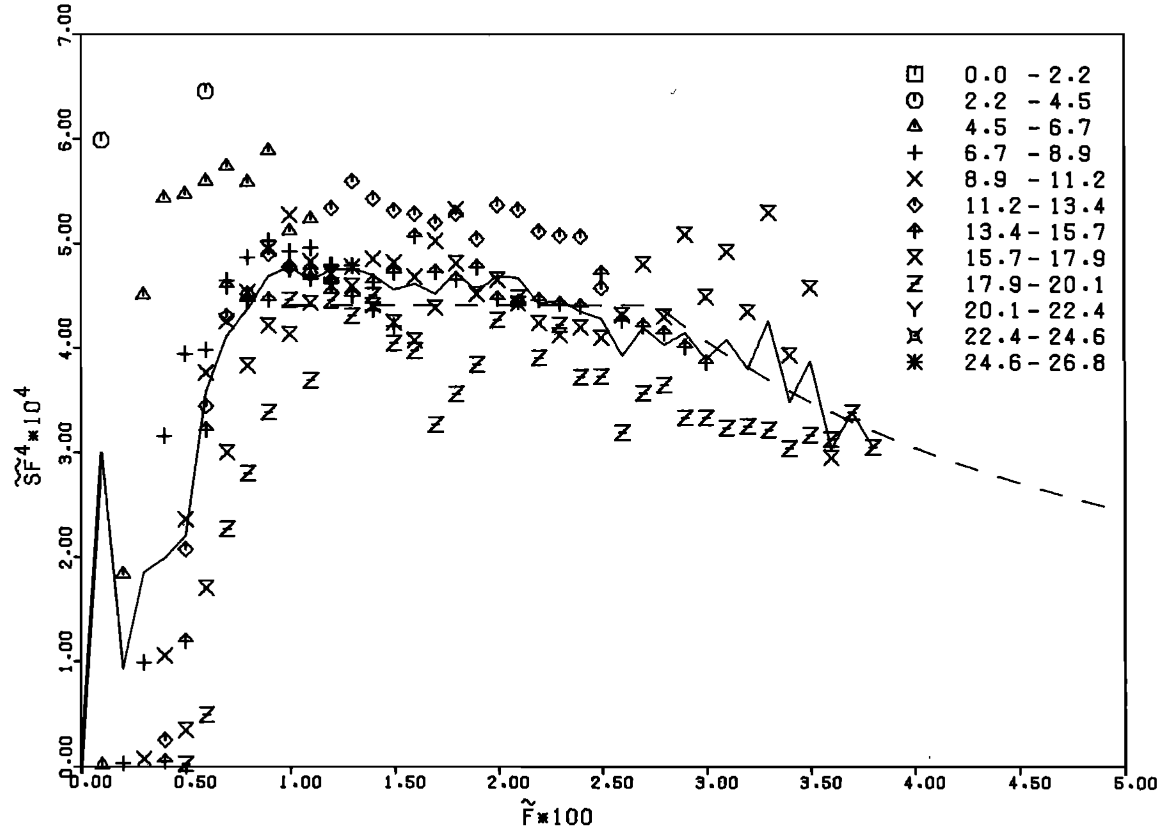

Fig. 5. Spectra times $\tilde{f}^4$ from Anita at Eugene Island 331. The symbols are for various wind speed categories in m/s. The solid line is the average of the data in frequency bands, and the dashed line is from equations (12) and (13).

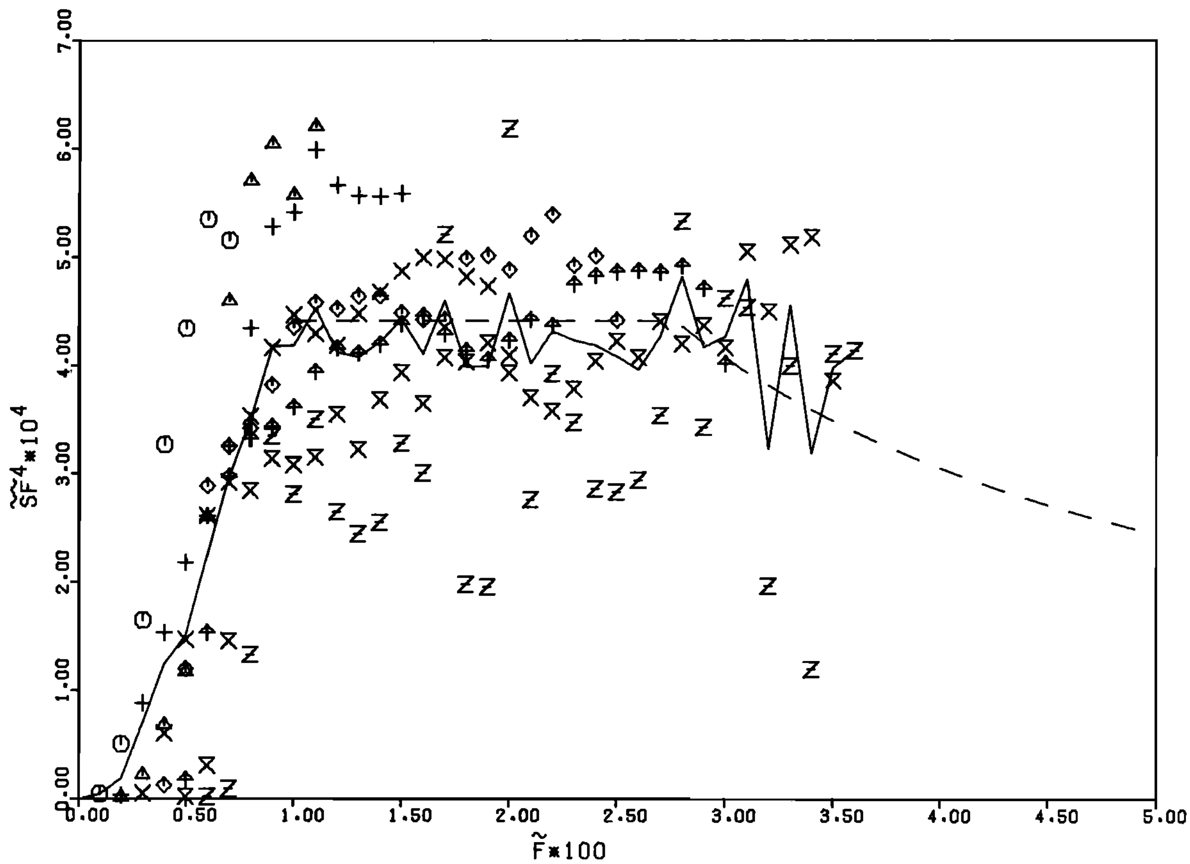

Fig. 6. Spectra times $\tilde{f}^4$ from Anita at Anita at South Pass 62. Legend as in Figure 5.

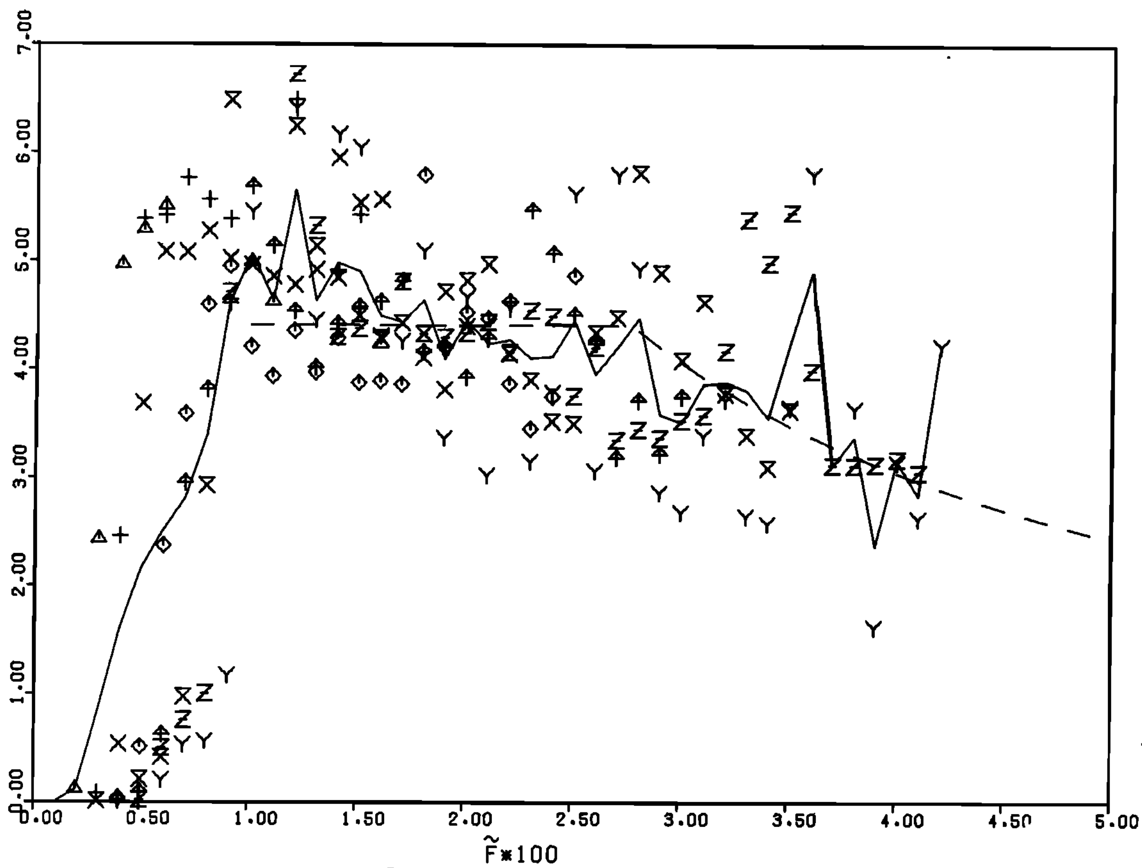

Fig. 7. Spectra times $\tilde{f}^4$ from Eloise at Eugene Island 331. Legend as in Figure 5.

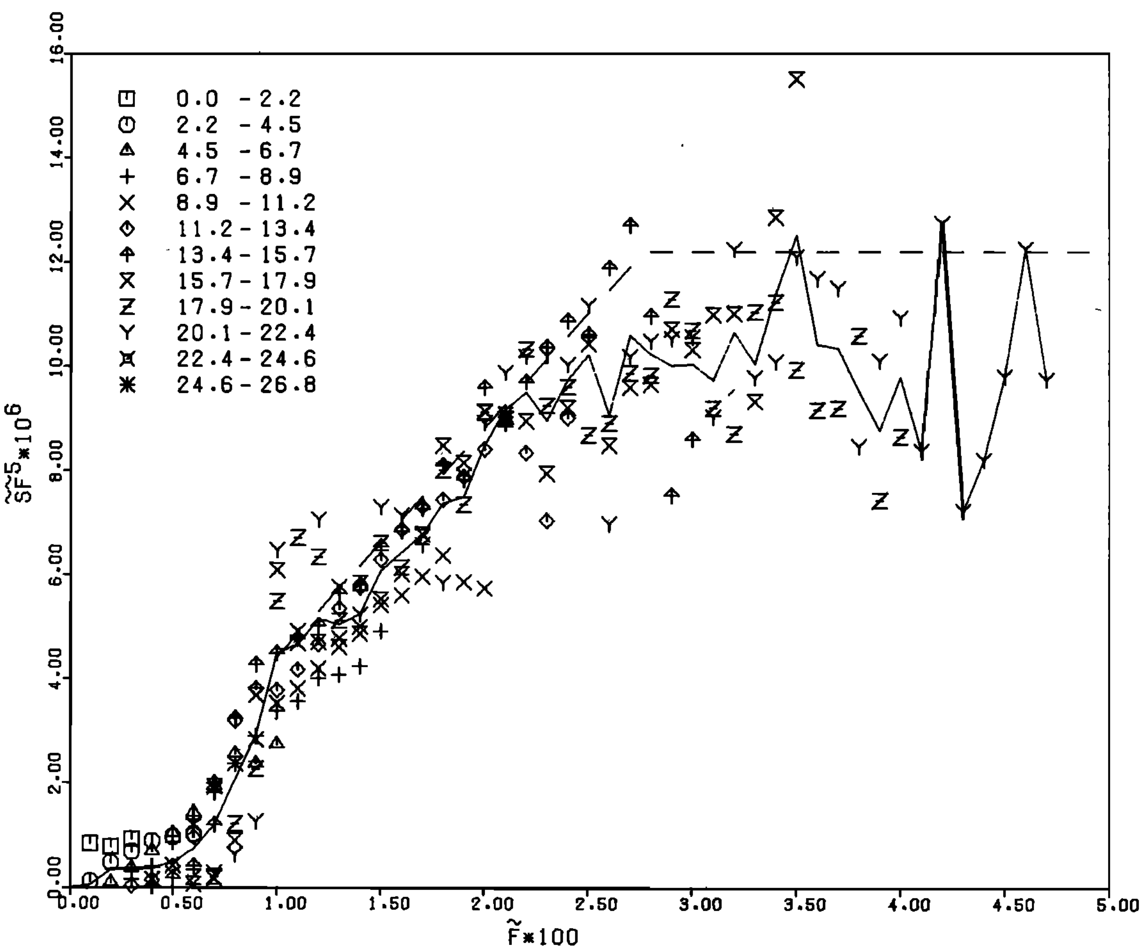

Fig. 8. Spectra times $\tilde{f}^5$ from the Pacesetter data. Legend as in Figure 5.

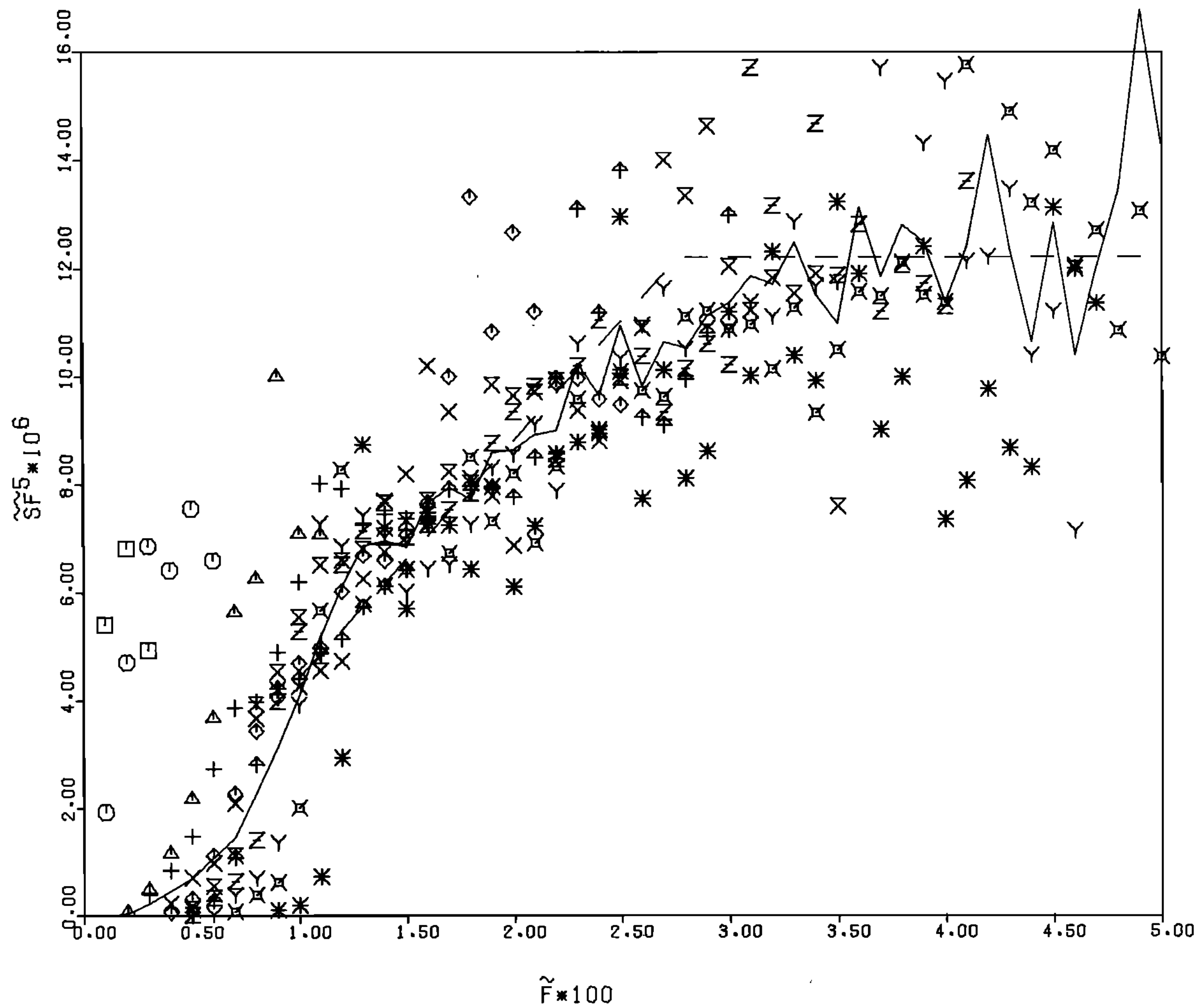

Fig. 9. Spectra times $\tilde{f}^5$ from Eloise at South Pass 62. Legend as in Figure 5.

The data in Figures 5–9 were averaged over frequency bands to produce the solid lines in the figures. It is again evident that the data can be described by two power law ranges. For $0.01 \leq \tilde{f} < 0.025$, the data is reasonably horizontal on the f^4 plots, while for $\tilde{f} > 0.03$, the data points dip on the f^4 plots, but are roughly horizontal on the f^5 plots. Since the data is reasonably fit by the two power law ranges, there seems little point in modifying a more complicated form such as (6) to fit the saturated range.

We are thus led to hypothesize that the saturated range actually consists of two subranges obeying different power laws. In particular, we propose that the saturated range has the form

$$\tilde{S}(f) = \alpha_4 \tilde{f}^{-4} \qquad \text{for} \qquad 0.01 < \tilde{f} < \tilde{f}_x \tag{12}$$

and

$$\tilde{S}(f) = \alpha_5 \tilde{f}^{-5} \qquad \text{for} \qquad \tilde{f} \geq \tilde{f}_x \tag{13}$$

where the coefficients α_4 and α_5 and the cross-over frequency $\tilde{f}_x$ were determined by further data averaging. The coefficient α_4 was obtained for each data set by averaging the data in the range $0.01 \leq \tilde{f} \leq 0.025$, and the coefficient α_5 came from averaging all the data with $\tilde{f} > 0.03$. The result of these calculations is shown in Table 3, along with overall averaged coefficients obtained by averaging the averages. The cross-over frequency was determined by setting (12) and (13) with the averaged coefficients equal to one another and solving to obtain

$$\tilde{f}_x = 0.0275 \tag{14}$$

Equations (12) and (13) with the overall averaged coefficients have been plotted as the dashed curves in Figures 5–9. The single curve provides a reasonable fit to all the data sets.

Since it has been generally accepted that the equilibrium range is reasonably well described by an $\tilde{f}^{-5}$ law, it is important to compare our results with those of previous investigators and attempt to explain the difference in conclusions.

Figure 4.8 in edition of *Phillips* [1977] is a well-known example of the type of data that has been offered in support of the $\tilde{f}^{-5}$ law. Spectra from several sources are plotted on a

TABLE 3. Average Equilibrium Range Coefficients

	α_4	α_5
Pacesetter	4.11×10^{-4}	10.09×10^{-6}
Eloise EI331	4.58×10^{-4}	12.91×10^{-6}
Eloise SP62	4.53×10^{-4}	12.42×10^{-6}
Anita EI331	4.59×10^{-4}	12.34×10^{-6}
Anita SP62	4.23×10^{-4}	13.24×10^{-6}
ODGP	4.53×10^{-4}	
Average	4.43×10^{-4}	12.20×10^{-6}

single log-log graph, and the tails of all the spectra are seen to be roughly asymptotic to a single line with slope equal to −5. Both laboratory and field data are included, and the scale for the dimensional spectra covers six decades. Taken together, the data are very convincing. However, the spectra from the individual sources, particularly those with the larger fetches, include reasonably broad ranges that might be better fitted by a −4 slope or by (6). In particular, the SWOP spectrum (shown in more detail by *Kinsman* [1965, p. 534]) approaches the f^{-5} curve very gradually and the fit is good only for frequencies above about three times that of the spectral peak.

As noted above, the dimensional analysis implies that a spectral range is independent of wind speed if and only if it is proportional to f^{-5}. It is thus very interesting that the fully developed spectra calculated by *Moskowitz* [1964] show a clear dependence on wind speed for all frequencies. *Pierson and Moskowitz* [1964] did not stress this feature in their proposal for a fully developed spectral form because of doubts about the accuracy at higher frequencies of the wave recorders used at that time.

Stacy [1974] did find wind speed dependence in his analysis of the high frequency tail of the spectrum during hurricane Camille. He proposed a rather complicated analytical form for the spectral range between 0.25 and 0.50 Hz, which unfortunately cannot be put in the nondimensional form discussed above. However, equations (12) and (13) seem to fit his data rather well.

Mitsuyasu et al. [1980] have recently given examples of spectra which fit a spectral form proposed by *Toba* [1973] that is equivalent to our (12). The average value of their coefficient corresponds to $\alpha_4 = 3.5 \times 10^{-4}$, with the value slightly dependent on fetch. They were also able to fit their spectra by using the JONSWAP parameterization. It is interesting that for frequencies above about twice that of the spectral peak, their data begins to rise above the JONSWAP fit. This is similar to the behavior in our Figure 2, although their figures only go up to $f/f_m = 3$.

It is unlikely that our observed wind speed dependent range was due to gross instrument errors, since the same sort of behavior was observed by using two quite different measurement systems. However, causes other than wind speed dependence have been suggested for the failure of an f^{-5} law. Kinsman discussed the possibility that peaks at the second harmonic frequency due to nonlinearity might distort the shape of the spectrum in that range if the main peak were narrow. However, second harmonic peaks were not evident in our individual spectra.

Phillips [1977, p. 147] points out that a surface current will cause a Doppler shift of the wave frequency measured at a fixed site. Current measurements were made during the hurricanes, and the current speed was usually below 0.5 m/s. Currents with speeds less than this could still distort the spectrum at frequencies on the order of 0.3 Hz, but the effect would increase with increasing frequency. Since we find agreement with an f^{-5} law at the highest frequencies, it seems likely that the effects must be averaged out due to varying directions between the waves and currents.

According to the dimensional analysis, the cause of the f^{-5} range is that the limiting form of the wave spectrum is dominated by wave breaking under the influence of gravity. The observational evidence is that there is an intermediate range of frequencies for which the wind speed also is important. Presumably, the spectral form in this region is influenced by the balance between energy input from the wind and resonant wave-wave interactions, as discussed by *Hasselmann et al.* [1973].

The value of $\alpha_5 = 12.20 \times 10^{-6}$ is higher than most previous estimates since it corresponds to $\alpha = 1.9 \times 10^{-2}$ in (11). The mean value of $\alpha = 1.5 \times 10^{-2}$ given by *Hasselmann et al.* [1973] is the highest listed by *Phillips* [1977, p. 147]. It is likely that the difference is due to different means of estimating the parameter. We used only the portion of the spectrum which clearly fits an f^{-5} dependence to determine α_5, while α was one of five parameters used by Hasselmann et al. to fit the shape of the entire spectrum. As shown in Figure 2, this can lead to an underestimate of the energy in the part of the spectrum that best follows an f^{-5} law. If α were determined by fitting an f^{-5} law to all frequencies above f_m, its value would be even lower.

Spectrum as a Function of Significant Wave Height and Mean Period

At some sites, information may be available about some features of the wave climate, such as scatter plots of significant wave height and mean periods. It would be useful to know whether such information would permit a more accurate specification of the spectrum than knowledge of the wind speed. First, it should be noted that an improved specification is unlikely for those data sets and frequencies that passed the KS test since the scatter of that data could be explained by natural statistical variability. However, the ODGP data set did not pass the test so those spectra were compared with significant wave heights and mean periods calculated from the wave records. The significant wave height was defined as the average of the highest one third of the zero downcrossing waves in the record and the mean period was the mean of the periods of all the waves in the record.

If the spectrum is a function of the significant wave height and mean period alone, then dimensional analysis gives a simple functional form for the spectrum. A nondimensional frequency can be defined by

$$\hat{f} = f/f_0 \tag{15}$$

where f_0 is the mean frequency that is the inverse of the mean period. The nondimensional spectrum is given by

$$\hat{S} = Sf_0/H_s^2 \tag{16}$$

and thus

$$\hat{S} = G(\hat{f}) \tag{17}$$

The measurements were converted to nondimensional form and then collected in 0.30 m significant height bins and averaged. The data sorted by height and period showed less scatter than when sorted by wind speed, but unfortunately it still failed the Kolmogorov-Smirnov test. This failure may have been caused by the presence of swell or fetch limitations.

The processed data is plotted on a log-log scale in Figure 10, where it is apparent that for frequencies greater than the mean frequency, all the measurements do collapse to a single function $G(\hat{f})$. Once again, it seems that the function is a power law with a slope of −4 on a log-log graph. No $\hat{f}^{-5}$ range appears in Figure 10, presumably because the nondimensional frequencies are never high enough in this data set. Averaging the data over $1.0 \le \hat{f} \le 2.5$ gave

$$\hat{S} = 0.051\hat{f}^{-4} \tag{18}$$

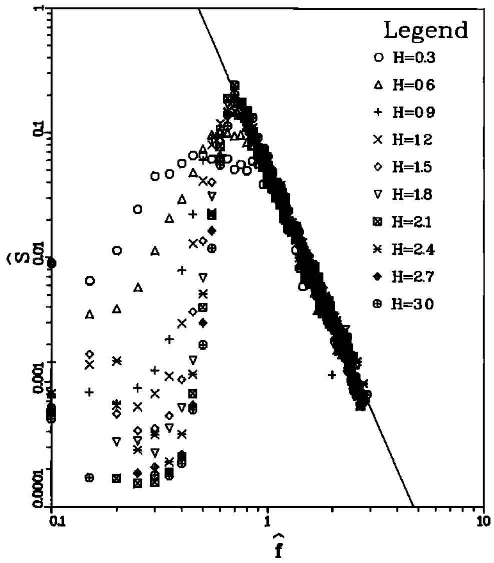

Fig. 10. ODGP spectra by significant wave height categories in meters. The solid line is from equation (18).

Conclusions

The wave spectra examined appear to have a large range that is in equilibrium with the local wind. By using simple nondimensional formulas, the spectral density in this saturated range can be accurately predicted given knowledge of the local wind friction velocity. For the lower frequency part of the range, the spectral density is proportional to the friction velocity and inversely proportional to the fourth power of the frequency, while for higher frequencies, an inverse fifth power law holds. Equations (12) and (13) express these relationships, and Table 3 lists the coefficients found for the various data sets. The saturated range spectrum can also be found given knowledge of the significant wave height and period.

The spectral densities calculated by using these formulas should be accurate compared with the natural variability that is expected in the random process. The accuracy and simplicity of the formulas should make them useful in engineering studies where predictions of the spectral density in the appropriate frequency range are needed.

Our data might also be fit by using the JONSWAP parameterization, possibly with an increase in the spectral density at frequencies several times that of the peak. However, the simpler forms proposed fit the measurements for a wide range of wind speeds and generating conditions with unknown, but, presumably, quite variable fetches.

Acknowledgments. The measurement programs on which this work is based involved the dedicated efforts of many people, including particularly R. C. Hamilton and T. E. Long. E. G. Ward and G. Rodenbusch made helpful comments on an earlier version of the manuscript.

References

Alexander, E., and R. C. Hamilton, A micro-processor based system for oceanographic data gathering, analysis and recording, Proceedings of the Offshore Technology Conference, Soc. of Petroleum Eng., Houston, 1978.

Forristall, G. Z., Wind and wave measurements from the first year of drilling in the Baltimore Canyon, Proceedings of the Offshore Technology Conference, Soc. of Petroleum Eng., Houston, 1980.

Forristall, G. Z., and R. C. Hamilton, Current measurement in support of fixed platform design and construction, Proceedings of a Working Conference on Current Measurement, NOAA, Office of Ocean Eng., University of Delaware, Newark, 1978.

Forristall, G. Z., J. R. Kreider, and A. M. Reece, Semisubmersible rig motion studies offshore of Alaska and southern California, *J. Energy Res. Tech., 101,* 182, 1979.

Forristall, G. Z., E. G. Ward, and V. J. Cardone, Wave kinematics and directional spectra in hurricanes Carmen and Eloise, Proceedings of the 17th International Conference on Coastal Engineering, Am. Soc. Civil Eng., Sydney, 1980.

Garratt, J. R., Review of drag coefficients over oceans and continents, *Mon. Weather Rev., 105,* 915–929, 1977.

Hamilton, R. C., and E. G. Ward, Ocean data gathering program: Quality and reduction of data, Proceedings of the Offshore Technology Conference, Soc. of Petroleum Eng., Houston, 1974.

Hasselmann, K., T. P. Barnett, E. Bouws, H. Carlson, D. E. Cartwright, K. Enke, J. A. Ewing, H. Gienapp, D. E. Hasselmann, P. Kruseman, A. Meerburg, P. Muller, D. J. Olbers, K. Richter, W. Sell, and H. Walden, Measurements of wind-wave growth swell decay during the Joint North Sea Wave Project (JONSWAP), Erganzungheft zur Deutsch. Hydrogr. Zeit., Hamburg, 1973.

Hoel, P. G., *Introduction to Mathematical Statistics,* John Wiley, New York, 1962.

Kinra, R. K., and P. W. Marshall, Fatigue analysis of the Cognac Platform, Proceedings of the Offshore Technology Conference, Soc. of Petroleum Eng., 1979.

Kinsman, B., Some evidence on the effect of nonlinearity on the position of the equilibrium range in wind-wave spectra, *J. Geophys. Res., 66,* 2411–2415, 1961.

Kinsman, B., *Wind Waves,* Prentice-Hall, Englewood Cliffs, N.J., 1965.

Kitaigorodskii, S. A., *The Physics of Air-Sea Interaction,* transl. from Russian, Israel Program for Scientific Translations, Jerusalem, 1973.

Mitsuyasus, H., F. Tasai, T. Suhara, S. Mizuno, M. Ohkusu, T. Honda, and K. Rikiishi, Observation of the power spectrum of ocean waves using a cloverleaf buoy, *J. Phys. Oceanogr., 10,* 286–296, 1980.

Moskowitz, L., Estimates of the power spectrum for fully developed seas for wind speeds of 20 to 40 knots, *J. Geophys. Res., 69,* 5161–5179, 1964.

Patterson, M. M., Oceanographic data from Hurricane Camille, Proceedings of the Offshore Technology Conference, Soc. of Petroleum Eng., Houston, 1974.

Phillips, O. M., *The Dynamics of the Upper Ocean,* Cambridge University Press, New York, 1977.

Pierson, W. J., and L. Moskowitz, A proposed spectral form for fully developed wind seas based on the similarity theory of S. A. Kitaigorodskii, *J. Geophys. Res., 69,* 5181–5190, 1964.

Stacy, R. A., Spectral analyses of high frequency gravity waves generated by a hurricane, Ph.D. thesis, School of Eng. and Sci., New York Univ., 1974.

Toba, Y., Local balance in the air-sea boundary process, III, *J. Oceanogr. Soc., Japan, 29,* 209–220, 1973.

Ward, E. G., Ocean data gathering program—An overview, Proceedings of the Offshore Technology Conference, Sponsor, Houston, 1974.

(Received November 7, 1980;
revised April 11, 1981;
accepted April 12, 1981.)